Clinical Oncology 34 (2022) 211–219

Contents lists available at ScienceDirect

Clinical Oncology

journal homepage: www.clinicaloncologyonline.net

Original Article

Clinical Implementation of Robust Multi-isocentric Volumetric Modulated Arc Radiotherapy for Craniospinal Irradiation

G. Smyth [*†], S. Mowat [‡], K. Chia [‡], K. Robinson [‡], K. Warren-Oseni [*], L.C. Welsh [‡], I. Blasiak-Wal [*], H.C. Mandeville [‡§]

[*] *Joint Department of Physics, The Institute of Cancer Research and the Royal Marsden NHS Foundation Trust, London, UK*
[†] *The London Radiotherapy Centre, HCA Healthcare UK, Guy's Hospital, London, UK*
[‡] *The Royal Marsden NHS Foundation Trust, London, UK*
[§] *The Institute of Cancer Research, London, UK*

Abstract

Aims: To determine if multi-isocentric volumetric modulated arc radiotherapy for craniospinal irradiation (CSI-VMAT) can be implemented safely and accurately using robust optimisation in a commercially available treatment planning system. Our initial clinical experience is reported for the first 20 patients treated with the technique.

Materials and methods: Patients received between 23.4 and 39.6 Gy (mode 23.4 Gy) in 13–22 fractions with CSI-VMAT. The heart mean dose was 4.2–10.3 Gy (median 5.3 Gy) for patients prescribed up to 24 Gy and 6.5–16.3 Gy (median 10.1 Gy) for patients receiving 35 Gy or more. The lung mean dose was 5.5–7.6 Gy (median 6.8 Gy) for patients prescribed up to 24 Gy and 6.9–11.1 Gy (median 10.0 Gy) for patients receiving 35 Gy or more. The robustness of the planning target volume $D_{0.1cm3}$ and $D_{99\%}$ to systematic errors in the isocentre superoinferior position of up to 5 mm was evaluated. These remained acceptable but were correlated to the length of the available beam overlap through the neck.

Results: As of January 2021, one patient was deceased after 508 days and one patient was lost to follow-up after completing treatment. The median follow-up was 399 days (range 175–756 days) and progression-free survival was 131 days (34–490 days). Acute toxicities at Common Terminology Criteria for Adverse Events v5.0 grade 3+ included lowered white blood cell count (16/20), decreased platelet count (8/20), nausea (5/20), vomiting (2/20), pharyngeal mucositis (1/20) and oral mucositis (1/20). Three patients developed grade 4 neutropenia or decreased white blood cell count.

Conclusions: CSI-VMAT can be implemented safely and accurately using robust optimisation functions in a commercially available treatment planning system.

Key words: Craniospinal irradiation; multi-isocentric; robustness; volumetric modulated arc therapy

Introduction

Radiotherapy to the whole craniospinal axis (craniospinal irradiation, CSI) requires the use of overlapping treatment fields due to the length of the combined planning target volume (PTV). This can be achieved using helical delivery, multiple isocentres with conformal radiotherapy (CRT) or intensity-modulated radiotherapy [1–7]. Modern intensity-modulated radiotherapy techniques, including multi-isocentric volumetric modulated arc therapy (VMAT), have been shown to reduce dose to organs at risk compared with CRT [8].

In multi-isocentric plans, patient positioning errors can cause substantial deviations from the planned dose if the separation between isocentres changes [9,10]. In CRT this is mitigated by using a moving ('feathered') junction and a dosimetrically equivalent approach is required during VMAT planning. Published work has relied on optimisation of the nominal plan or individual beam contributions to achieve sufficient robustness [9,11]. However, robust optimisation techniques quantify the effect of simulated errors directly during planning and adjust the nominal plan to improve the worst-case scenario. Using robust optimisation in CSI could achieve both the high-quality dosimetry of VMAT and the required robustness to set-up errors.

Here we report the clinical implementation of a multi-isocentric VMAT technique for CSI that accounts for up to 27 error scenarios using robust optimisation. We describe

Author for correspondence: H.C. Mandeville, The Royal Marsden NHS Foundation Trust, Downs Road, Sutton, London, SM2 5PT, UK.
E-mail address: henry.mandeville@rmh.nhs.uk (G. Smyth).

https://doi.org/10.1016/j.clon.2022.01.004

our initial clinical experience based on the first 20 patients treated with this technique, including the robustness of the final clinical plans to simulated patient set-up errors, and their delivery accuracy. Finally, we report acute toxicities, progression-free survival (PFS) and overall survival recorded during patient follow-up to date.

Materials and Methods

Following institutional review board approval, a retrospective review was undertaken of the first 20 paediatric, adolescent and adult patients treated with CSI-VMAT at The Royal Marsden Hospital since the clinical implementation of the technique in May 2019.

Patient Immobilisation and Computed Tomography Scanning

Patients were positioned supine and immobilised using a five-point thermoplastic shell and head rest. An indexed knee pad immobilised the legs, ensured a reproducible pelvic tilt and minimised anteroposterior curvature of the spine. Arms were extended, resting alongside the thighs, and the distance from the tip of each middle finger to the knee pad was recorded to guide set-up at treatment. Computed tomography (CT) markers, and tattoos or shell marks, were placed midline at the superior skull, superior spine, mid-spine and inferior spine. Lateral CT markers were placed at the mandible and pelvis. Patients were scanned on a SOMATOM Emotion large bore CT scanner (Siemens Healthcare GmbH, Erlangen, Germany), with 2 mm slice spacing along the whole craniospinal axis. An additional brain reconstruction with 1.5 mm slice spacing was used to guide intracranial contouring and for planning the subsequent boost phase.

Treatment Planning

Target Volume Definition

Spinal and whole-brain clinical target volumes (CTV_Spine and CTV_WB, respectively) were contoured with reference to SIOPE consensus guidelines [12]. The cribriform plate was directly included within CTV_WB, as recommended [12]. The bilateral optic nerves, defined as CTV, were delineated separately to aid treatment planning. CTV_WB and the bilateral optic nerves were combined and expanded uniformly by 3 mm to define the whole-brain PTV (PTV_WB). CTV_Spine was divided into cervical, thoracic and lumbar-sacral sections (CTV_Cervical, CTV_Thoracic, and CTV_Lumbar) to allow variation in CTV-PTV margins. Spinal margins were informed by local protocols for similar clinical sites and the potential for increased error inferiorly, with 7 mm applied uniformly to CTV_Cervical and CTV_Thoracic, and 10 mm applied uniformly to CTV_Lumbar. The union of the spine PTVs with PTV_WB gave PTV_Combined. A prescription volume, PTV_Prescribe, was created by contracting PTV_Combined from the patient contour by 5 mm to exclude the build-up region.

Patients still growing also had a CTV defined that encompassed the vertebral bodies (VB_Adjacent), used to ensure uniform bone growth after treatment [13]. No CTV–PTV margin was added to the VB_Adjacent volume. All target volumes are summarised in Supplementary Table S1.

Treatment Beam Geometry

Treatment planning was carried out in RayStation (v8A & v9A, RaySearch, Stockholm). Each plan comprised partial VMAT arcs at two or three isocentres in the brain, superior spine and inferior spine (Figure 1). Where possible, the brain isocentre was placed at the localisation point defined by shell markers so that no shifts were required. Subsequent isocentres were positioned to ensure that only longitudinal couch translations were required to move between isocentres. One partial arc primarily treated the brain, three partial arcs primarily treated the superior spine and three partial arcs primarily treated the inferior spine. In paediatric cases, three partial arcs were used to treat the whole spine with an isocentre positioned mid-spine.

Beams from adjacent isocentres overlapped in the neck and mid-spine. Long junctions, particularly in the mid-spine, were permitted to allow dosimetric feathering during optimisation. The inferior extent of the brain field was restricted, to avoid entering through the arms and shoulders. The maximum superior extent of the superior spine fields was restricted to avoid entering through the jaw and to ensure overlap with the brain field was only through the cervical spine where possible. Gantry start and stop positions for each partial arc were set to avoid areas of increased uncertainty in patient positioning or beam attenuation. In the spine, beams avoided entering through the arms, whereas the brain arc avoided entering through a highly attenuating region of the couch.

Treatment Plan Optimisation

During optimisation, attempts to reduce the dose to the lenses were carried out with caution to prevent underdosing the cribriform plate, which can cause relapse [14]. An additional optimisation structure, which included the PTV around the cribriform plate and optic nerves, was used to ensure coverage in this high-risk area (Supplementary Figure S1). A visual review of the dosimetry in this region was also carried out by the consultant clinical oncologist during plan approval. A dose fall-off objective was applied beyond the combined PTV to encourage conformity of the high and intermediate doses unconstrained by organ at risk objectives. Additional non-anatomical structures were used to reduce low and intermediate dose to normal tissue, including the facial bones, oral cavity and abdomen. Plans were calculated on a 2.5 mm $\times$ 2.5 mm $\times$ 2.5 mm dose grid using a Collapsed Cone algorithm and prescribed to give a median dose to the PTV_Prescribe. Additional objectives were added to achieve a minimum dose to VB_Adjacent dependent on prescription, in line with SIOPE recommendations for vertebral body dose management [13].

Robust optimisation objectives were added to mitigate the effect of superior–inferior set-up errors using the robustness options in RayStation. Robust objectives for

minimum dose to CTV_Spine and maximum dose to PTV_Spine were included. Shifts of 5 mm in the superior and inferior directions were simulated independently during optimisation for each isocentre to compute the impact of nine or 27 combinations for a two- or three-isocentre VMAT plan. Additional set-up errors were incorporated in CTV–PTV margins, as standard.

Delivery Preparation

After completion, the plan was separated into individual 'beam set' plans to allow dose recording in Mosaiq (Elekta, Crawley, UK) and safe reference image set-up for image matching at each isocentre. As well as reference volumetric images, reference digitally reconstructed radiographs were created for a lateral beam at the brain isocentre and an anterior beam for each spine isocentre.

Robustness Evaluation

To confirm that the nominal plan was sufficiently robust, systematic errors in the superior–inferior direction were simulated. The superior spine isocentre position was adjusted by 5 mm superiorly, bringing it closer to the brain isocentre. The perturbed plan dose was calculated by combining the original brain and inferior spine beam sets with the perturbed superior spine beam set. This was repeated for a superior isocentre shift of 3 mm and inferior shifts of 3 and 5 mm. Systematic error simulation and evaluation was repeated for the inferior spine isocentre, where present for three isocentre plans. Perturbed plan doses were assessed based on clinical goals agreed for error simulated plans and visually compared against the clinical plan and the location and size of hot and cold spots in the event of systematic uncertainties were assessed.

Variations from the nominal plan in near maximum ($D_{0.1cm3}$) and near minimum ($D_{99\%}$) doses with systematic shifts were tested for correlation with neck junction length using the Pearson correlation coefficient in Excel (Microsoft, Washington, USA).

Delivery Quality Assurance

Pre-treatment delivery quality assurance (DQA) was carried out using a Delta4 diode array (ScandiDos AB, Uppsala, Sweden) [15]. The patient plan for each isocentre was calculated on the Delta4 phantom with a dose grid of 2 mm × 2 mm × 2 mm. If beams were longer than the 20 cm measurement region, the inferior section was measured in the standard orientation, then the superior section was measured with the Delta4 rotated by 180° to avoid irradiating its electronics. Therefore, up to six measurements were carried out for each case. Clinical DQA tolerance required at least 95% of detectors receiving >20% of the dose should have a gamma <1, using 3% of the global dose maximum and 3 mm distance to agreement criteria ($\gamma_{3G/3}$).

Imaging and Treatment Protocol

Patient Positioning

A surface rendered view and surface measurements between each anterior tattoo or shell mark were used to confirm positioning before the couch was shifted to align the localisation point with the room lasers.

Fraction One

On fraction one, all isocentres were imaged prior to delivery of any beams to identify and remove any gross geometric errors. The brain and superior spine isocentre position was verified by acquiring a planar kilovoltage (kV) image for comparison against a reference digitally reconstructed radiographs with an action tolerance of 2 mm. If no correction was required, the next isocentre was verified. A conebeam CT (CBCT) scan was acquired to confirm the

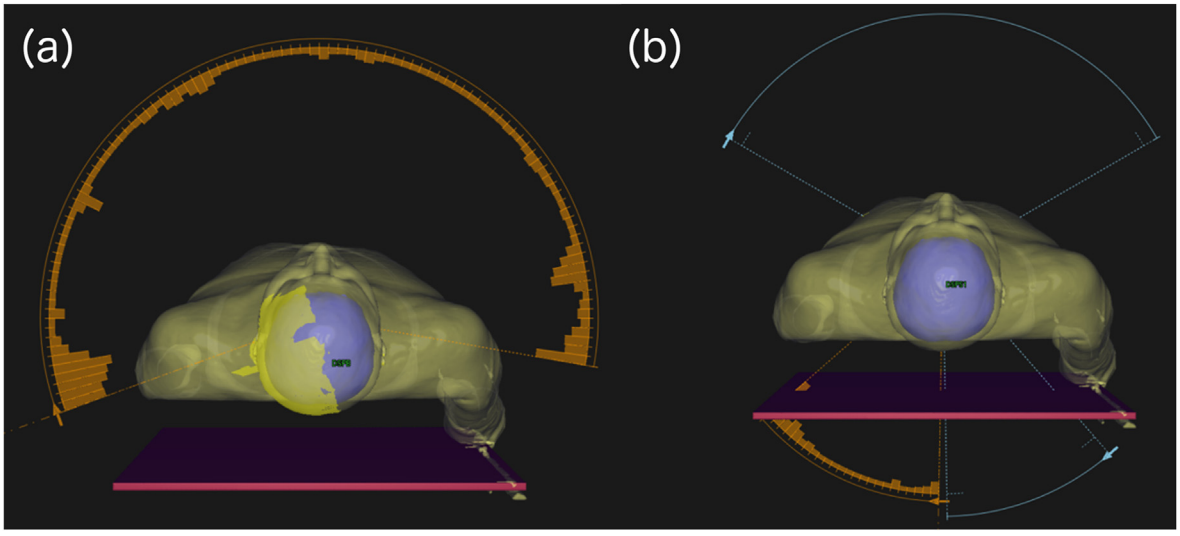

Fig 1. Beam orientations for (a) the partial arc used to treat the brain and neck while avoiding treatment through a highly attenuating superior section of the treatment couch and (b) the partial arcs used at each spine isocentre used to treat the spine (and neck for the superior spine) while avoiding treatment through the arms and shoulders.

position of the inferior spine isocentre and quantify any displacement or rotation. Rotations $\geq 3^{\circ}$ triggered correction of the pelvic alignment by manual manipulation or re-set-up of the patient, confirmed using a repeat CBCT.

Subsequent isocentres were then imaged using CBCT prior to delivery. For each isocentre, the patient was realigned to the localisation point, shifted to the superior spine isocentre and a pre-treatment CBCT was acquired.

Subsequent Fractions

Pre-treatment CBCT imaging was carried out on fractions two and three. As the pelvis has the most potential for rotation, the inferior spine was imaged and treated first. Images were acquired at each isocentre before treatment and corrected with an online no action level protocol.

Systematic error analysis and correction was carried out after fraction three, and the frequency of subsequent imaging was decided in discussion with the multidisciplinary team. A complete set of imaging was acquired at least once a week to monitor the relative position of adjacent isocentres. Daily imaging of the inferior spine using kV planar imaging was allowed to check alignment.

Clinical Follow-up

Patients were followed up as part of their normal care. PFS, defined as the time from the last fraction of radiotherapy to the most recent magnetic resonance imaging scan without progression, and overall survival, defined as the time from the date of diagnosis until the end of analysis (8 January 2021), were monitored. A series of reported acute side-effects were graded on the Common Terminology Criteria for Adverse Events (CTCAE) v5.0 scale. These were: fatigue, skin reactions (radiation dermatitis, alopecia), gastrointestinal toxicity (pharyngeal mucositis, oral mucositis, dysgeusia, nausea, vomiting, gastroesophageal reflux disease, diarrhoea, constipation), haematological toxicity (decreased white blood cell count, neutropenia, anaemia, decreased platelet count) and neurological effects (headache, photophobia).

Results

Clinical Implementation

CSI-VMAT was implemented clinically in May 2019 and 20 patients with a median age of 8 years (range 3–32 years) were treated within the first 18 months the service was available. Patients were prescribed doses between 23.4 and 39.6 Gy (mode 23.4 Gy) in 13–22 fractions with CSI-VMAT according to diagnosis, followed by a VMAT boost to the tumour bed and any metastases of 30.6 Gy (14.4–30.6 Gy). The median PTV length was 60.6 cm (range 46.8–75.6 cm) and 12 patients required three isocentres. Three patients were replanned prior to starting radiotherapy due to significant anatomical differences from their planning CT. One patient triggered a replan partway through treatment, changing plan from fraction 11 of 20. Demographic and treatment details for all patients are presented in Table 1, and dose distributions for a representative patient are presented in Figure 2.

The near-minimum dose ($D_{99\%}$) to PTV_Prescribe was 96.1–97.9% (median 96.5%) of the prescribed dose. PTV_Spine and PTV_WB received near-minimum doses ($D_{99\%}$) of 95.4–97.5% (96.1%) and 94.5–98.1% (96.5%), respectively. For patients prescribed up to 24 Gy, the heart mean dose was 4.2–10.3 Gy (median 5.3 Gy), the lung mean dose was 5.5–7.6 Gy (6.8 Gy), lung V_{20Gy} was 0.5–4.7% (1.7%), lung V_{5Gy} was 41.8–49.7% (46.8%), left kidney mean dose was 2.3–8.6 Gy (6.3 Gy), right kidney mean dose was 4.6–11.8 Gy (6.8 Gy) and liver V_{19Gy} was 0.0–2.7% (0.1%). For patients receiving 35 Gy or more, the heart mean dose was 6.5–16.3 Gy (10.1 Gy), the lung mean dose was 6.9–11.1 Gy (10.0 Gy), lung V_{20Gy} was 3.5–23.7% (15.3%), lung V_{5Gy} was 47.0–67.5% (50.4%), left kidney mean dose was 5.0–14.0 Gy (9.9 Gy), right kidney mean dose was 7.9–14.2 Gy (11.4 Gy) and liver V_{19Gy} was 2.0–35.1% (7.2%). Key dose statistics for all patients are shown in Figure 3 and Supplementary Figure S2.

Robust Evaluations

Robust evaluation results for all patients are shown in Figure 4. There were very strong correlations between neck junction length and the reduction in PTV_Spine $D_{99\%}$ from the nominal plan with 3 mm and 5 mm shifts of the superior spine isocentre inferiorly (Pearson's r values of 0.86 and 0.90, respectively). There were strong ($r = -0.64$) and moderate ($r = -0.57$) inverse correlations between neck junction length and PTV $D_{0.1cm3}$ for 3 mm and 5 mm superior shifts, respectively. Full results are presented in Supplementary Figures S3–S7.

Delivery Quality Assurance

DQA was carried out for the first 16 patients and all measurements passed local clinical tolerances with 95.2–100% (median 99.8%) of detectors passing $\gamma_{3G/3} < 1$. The process was then streamlined, with DQA only if requested after an independent monitor unit check using RadCalc (LifeLine Software Inc., Texas, USA).

Clinical Follow-up

As of January 2021, one patient was deceased after 508 days, and one patient was lost to follow-up after treatment completion. The median time from the date of diagnosis to the end of treatment was 81.5 days (range 69–140 days). After a median follow-up of 399 (175–756) days, the median overall survival was 399 (175–756) days and PFS was 131 (34–490) days. For the subset of patients initially diagnosed as standard-risk medulloblastoma, after a median follow-up of 275 (175–639) days, overall survival was 275 (175–639) days and PFS was 129 (34–457) days. However, two patients initially diagnosed as standard risk were reclassified as high risk after radiotherapy. Acute toxicities at CTCAE v5.0 grade 3+ included lowered white

Table 1
Summary of patient diagnoses, craniospinal irradiation (CSI) prescription doses and treatment planning technique

Case	Diagnosis	Chemotherapy	CSI prescription		PTV length (cm)	No. isocentres
			Dose (Gy)	Fractions		
1	Medulloblastoma	No	23.4	13	67.4	3
2	Medulloblastoma (m)	Yes	36.0	20	46.8	2
3	Pineoblastoma (m)	Yes	39.6	22	52.0	2
4	Choroid plexus carcinoma	No	35.0	21	75.4	3
5	Medulloblastoma	No	23.4	13	71.4	3
6	Medulloblastoma (m)	Yes	36.0	20	61.8	3
7	Medulloblastoma	No	23.4	13	53.6	2
8	High grade neuroepithelial tumour	No	36.0	20	69.7	3
9	Medulloblastoma (m)	Yes	36.0	20	53.4	2
10	Medulloblastoma	No	23.4	13	52.4	2
11	Germinoma (m)	No	24.0	16	61.4	3
12	Medulloblastoma	No	23.4	13	56.2	2
13	Medulloblastoma	No	23.4	13	57.2	3
14	Medulloblastoma	No	23.4	13	66.4	3
15	Medulloblastoma (m)	No	39.6	22	59.8	3
16	Medulloblastoma (m)	Yes	36	20	65.8	3
17	Medulloblastoma (HR)	Yes	36	20	53.2	2
18	Medulloblastoma	No	23.4	13	73.8	3
19	Medulloblastoma (m)	No	39.6	22	55.6	2
20	Medulloblastoma	No	23.4	13	64.2	3

HR, high risk; m, metastatic; PTV, planning target volume.

blood cell count (16/20), neutropenia (13/20), nausea (5/20), decreased platelet count (8/20), vomiting (2/20), pharyngeal mucositis (1/20) and oral mucositis (1/20). Three patients presented with grade 4 neutropenia or lowered white blood cell count, one of whom reported both. Reported acute toxicities by CTCAE grade are summarised in Table 2.

Discussion

Craniospinal VMAT using robust optimisation has been implemented successfully in our clinic. By evaluating the clinical plans for the first 20 patients treated, we have shown that this technique achieves both high-quality dosimetry in the nominal plan and clinically acceptable

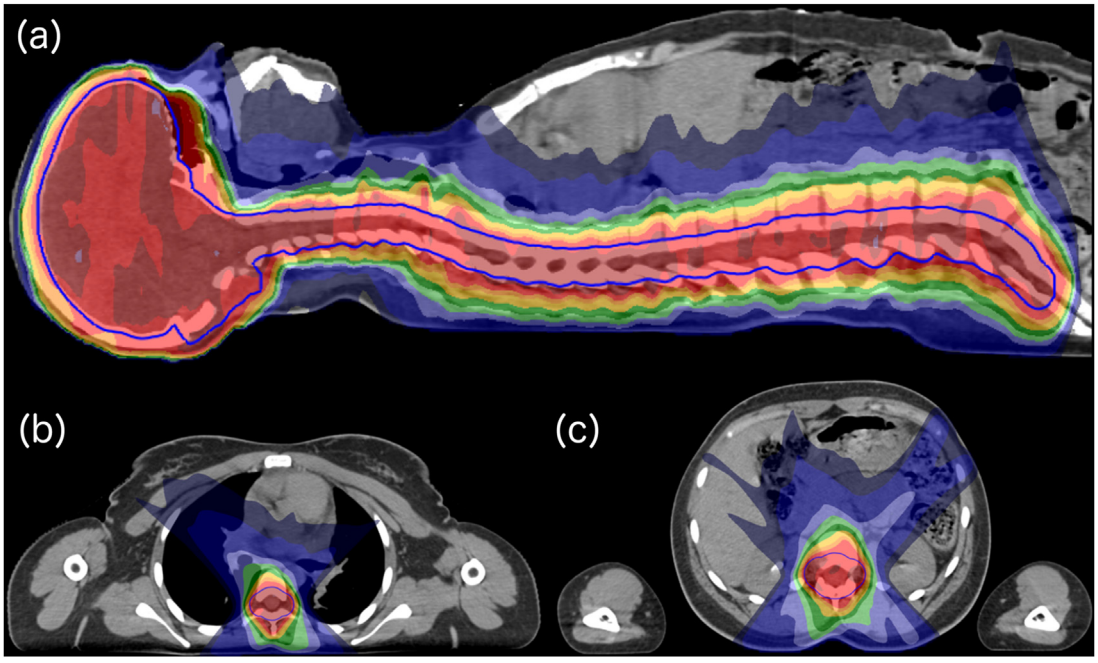

Fig 2. Dose distributions for (a) sagittal view through the centre of the planning target volume, (b) axial view at the level of the heart and (c) axial view at the level of the kidneys.

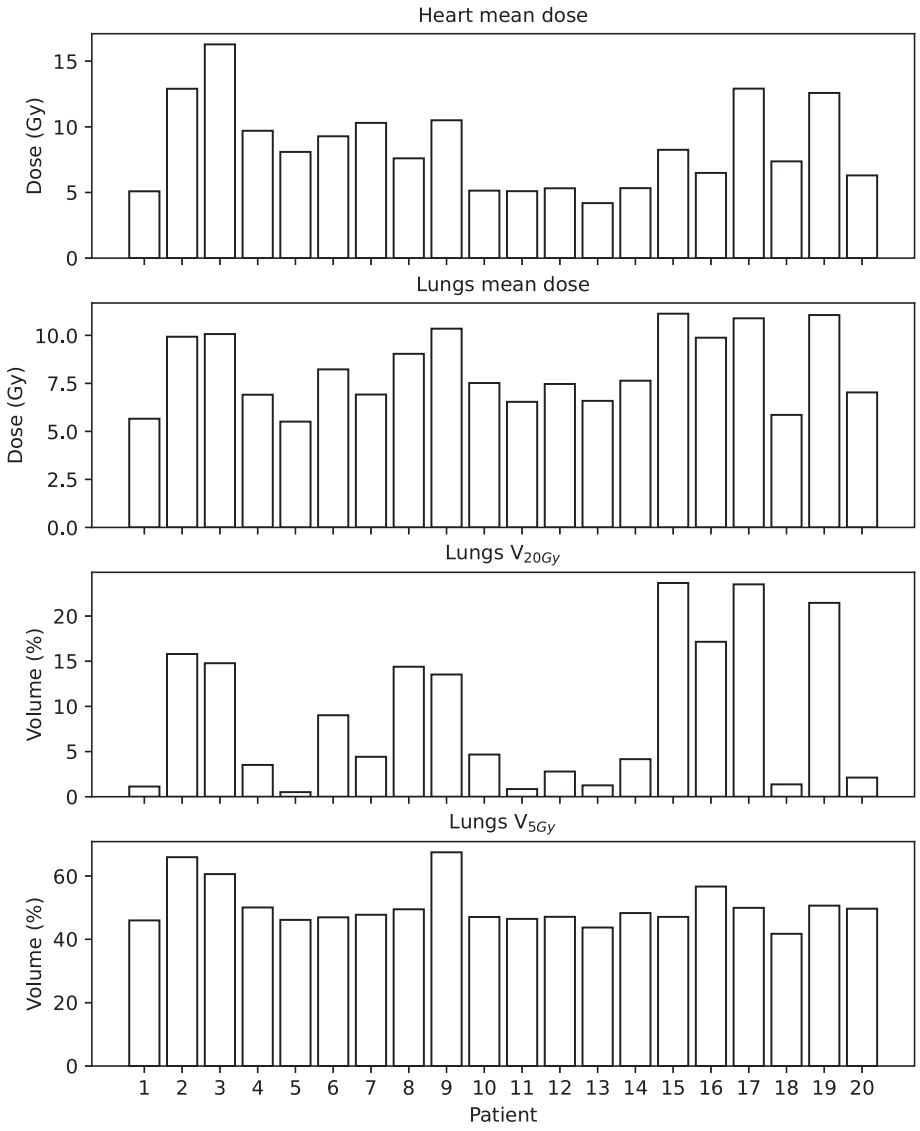

Fig 3. Nominal plan heart mean dose, lung mean dose, lung V_{20Gy} and lung V_{5Gy} dose statistics for all patients.

robustness to simulated systematic errors of up to 5 mm. Neck junction length was found to be correlated with the increase in near maximum dose under error, suggesting that shoulder and jaw position at immobilisation and beam overlap definition at planning are important. The delivery accuracy of the clinical plans was sufficiently high that pre-treatment DQA could be streamlined after 16 cases. Although patients experienced a number of acute side-effects, these were in line with expectations for this cohort, which included patients with high-risk or metastatic disease receiving higher CSI doses and concomitant daily carboplatin chemotherapy. Statements of PFS and overall survival over the analysis period are included for completeness and we acknowledge that the follow-up period was not sufficient for an accurate inference of their true values. PFS and overall survival data for these patients will continue to be collected. However, reported follow-up to date is in line with expectations.

Myers *et al.* [9] evaluated the robustness of five CSI cases planned using a 'gradient optimised' VMAT technique. Their results compare favourably to the inferior spine isocentre perturbation results in this paper, which are most similar in overlap region. The robustness in the neck region was not evaluated. However, the effect of beam pathlength changes with isocentre position in this region would not have been accounted for. We also mitigated for variation in arm position by using partial arcs, rather than the 358° arcs used by Myers *et al.* [9]. Wang *et al.* [11] proposed a 'staggered' optimisation technique for three-isocentre CSI-VMAT to improve robustness with several fixed beam lengths, similar to a moving junction in CRT. Although not directly comparable with our results, neck junction PTV and mid-spine junction PTV near maximum doses ($D_{2\%}$) were 115.7–127.0% for 5 mm shifts of the superior spine isocentre depending on junction length.

Comparing acute toxicity results with published reports for comparable techniques is challenging due to differences

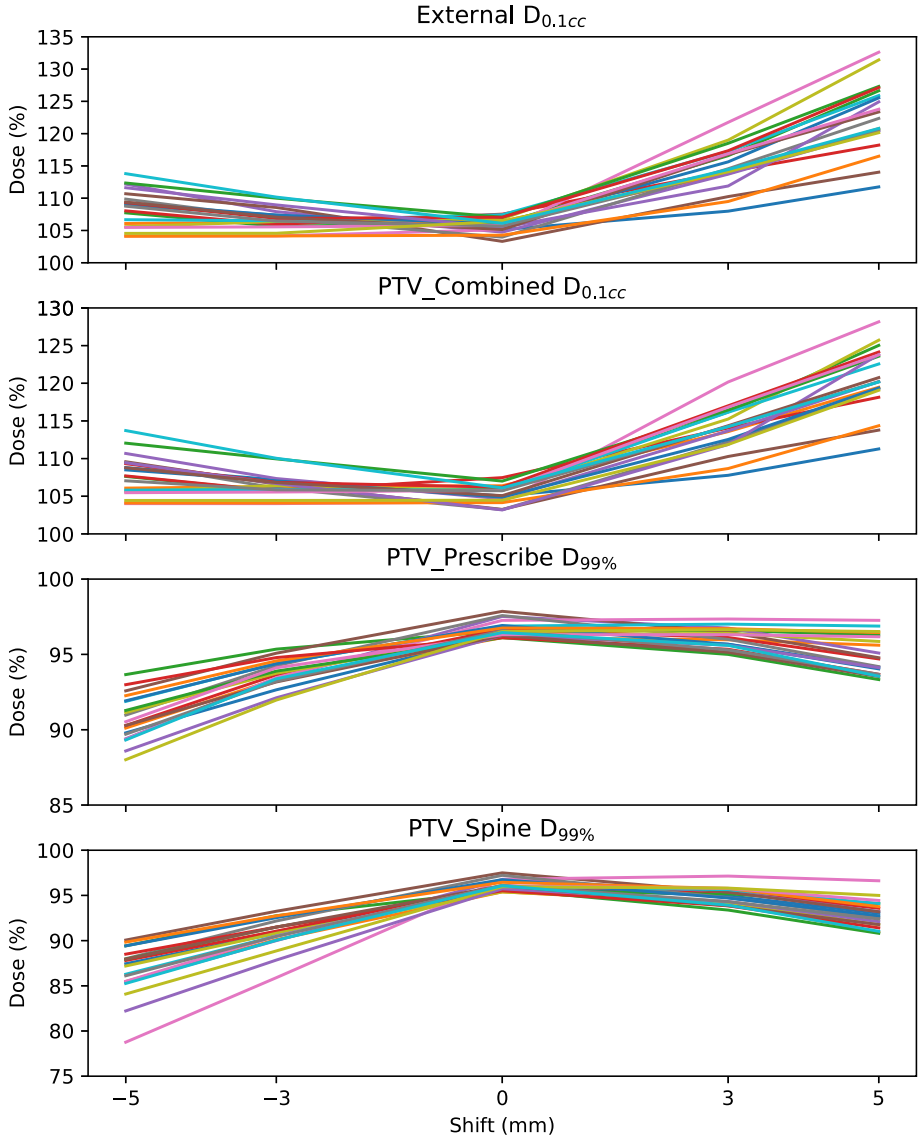

Fig 4. Robustness of near minimum ($D_{99\%}$) and near maximum ($D_{0.1cm3}$) dose statistics to simulated systematic shifts of the superior spine isocentre in the superoinferior direction. Dose values are relative to prescription for each case. Superior shifts are positive; zero shifts indicate the nominal plan.

in diagnosis, prescription dose and chemotherapy use between cohorts. Penagaricano *et al.* [16] treated 18 paediatric patients to a higher modal dose of 36 Gy with Tomotherapy. They recorded less nausea (CTCAE v3, grade 1 4/18, grade 2 6/18) but more vomiting (grade 1 1/18, grade 2 4/20) and weight loss (grade 1 6/18, grade 2 8/18). Two patients died during the follow-up period (median 16.5 months). Wong *et al.* [17] treated 19 paediatric patients with CSI-VMAT planned without robust optimisation. All patients had leukopenia (CTCAE V4, grade 2 2/19, grade 3 5/26, grade 4 12/19) and most had thrombocytopenia (grade 1–2 3/19, grade 3 5/19, grade 4 7/19). They reported higher rates of weight loss (grade 1 9/19, grade 2 5/19) and more frequent grade 2 anaemia (17/19). Overall, acute toxicity results reported here appear to be in line with the literature.

Proton therapy will probably further reduce the dose to the heart and lungs, even compared with advanced photon techniques [8]. The incidence of symptomatic late cardiac toxicity and its correlation with plan dosimetry has been evaluated in the Childhood Cancer Survivor Study [18,19]. Excess risk of cardiac events is correlated with heart mean dose greater than 10 Gy, V_{20Gy} of 0.1% or more and V_{5Gy} of 50% or more for patients receiving a heart maximum dose <20 Gy. In a phase II clinical trial, Yock *et al.* [20] did not see any late cardiac or lung toxicity in 59 paediatric and young adult patients treated with proton therapy for medulloblastoma after a median follow-up of 7 years. These results suggest that proton therapy could reduce the risk of late cardiac toxicity compared with photons, particularly for high-risk cases where the prescribed dose to the whole craniospinal axis is greater [21].

A limitation of this work is that robust optimisation for photon treatment planning is not currently available in all commercial treatment planning systems. However, it is

Table 2
Summary of acute toxicities by Common Terminology Criteria for Adverse Events (CTCAE) v5 grade for all patients

Acute toxicity	CTCAE v5 grade				
	1	2	3	4	Any
Fatigue	10	4	0	0	14
Radiation dermatitis	8	8	0	0	16
Alopecia *	2	17	0	0	19
Pharyngeal mucositis	8	3	1	0	12
Oral mucositis	2	1	1	0	4
Dysgeusia	5	2	0	0	7
Nausea	5	6	5	0	16
Vomiting	11	1	2	0	14
GERD	1	3	0	0	4
Diarrhoea	5	0	0	0	5
Constipation	7	2	0	0	9
Weight loss *	5	1	0	0	6
Headache	4	0	0	0	4
Photophobia	1	0	0	0	1
WBC decreased	0	3	14	2	19
Neutropenia	2	4	11	2	19
Anaemia	6	11	0	0	17
Platelet count decreased	9	2	8	0	19

GERD, gastroesophageal reflux disease; WBC, white blood cell count.
* Data unavailable for one patient for alopecia and weight loss.

widely available for proton planning so could be implemented in response to clinical demand. Where robust optimisation tools for photon planning are not currently available, the results presented here can be used to help evaluate perturbations of a nominal multi-isocentric plan. The time required for robust planning was longer than for a conventionally optimised plan due to the number of error combinations evaluated. Despite the complexity, optimisation times were not prohibitive in a busy clinical department when using the graphic processor unit for dose calculation.

Despite the increasing focus on proton therapy for CSI, its cost and availability will probably limit access in many countries. Meanwhile, centres treating CSI with CRT must maintain staff competence and patient safety for extended source to surface distance techniques as experience with their use declines. These issues suggest that a multi-isocentric VMAT technique, sufficiently robust to patient positioning errors, has a place in future CSI treatment. Further work to refine the CSI-VMAT technique is planned, including prospective investigation of local set-up data and its impact on PTV margins, and a national audit of immobilisation and imaging techniques for CSI.

Conclusion

Multi-isocentric VMAT for CSI can be implemented safely and accurately using robust optimisation in a commercially available treatment planning system.

Conflicts of interest

The authors declare no conflict of interest.

Acknowledgements

This paper represents independent research funded by the NIHR Biomedical Research Centre at The Royal Marsden and The Institute of Cancer Research. The views expressed are those of the authors and not necessarily those of The Royal Marsden Hospital and The Institute of Cancer Research.

Appendix A. Supplementary data

Supplementary data to this article can be found online at https://doi.org/10.1016/j.clon.2022.01.004.

References

[1] Wilkinson JM, Lewis J, Lawrence GP, Lucraft HH, Murphy E. Craniospinal irradiation using a forward planned segmented field technique. *Br J Radiol* 2007;80:209–215. https://doi.org/10.1259/bjr/61306844.
[2] Bauman G, Yartsev S, Coad T, Fisher B, Kron T. Helical tomotherapy for craniospinal radiation. *Br J Radiol* 2005;78:548–552. https://doi.org/10.1259/bjr/53491625.
[3] Sharma DS, Gupta T, Jalali R, Master Z, Phurailatpam RD, Sarin R. High-precision radiotherapy for craniospinal irradiation: evaluation of three-dimensional conformal radiotherapy, intensity modulated radiation therapy and helical Tomotherapy. *Br J Radiol* 2009;82:1000–1009. https://doi.org/10.1259/bjr/13776022.
[4] Myers P, Stathakis S, Gutiérrez AN, Esquivel C, Mavroidis P, Papanikolaou N. Dosimetric comparison of craniospinal axis irradiation (CSI) treatments using helical Tomotherapy, Smartarc, and 3D conventional radiation therapy. *Int J Med Phys Clin Eng Radiat Oncol* 2013;2:30–38. https://doi.org/10.4236/ijmpcero.2013.21005.
[5] Bedford JL, Lee YK, Saran FH, Warrington AP. Helical volumetric modulated arc therapy for treatment of craniospinal axis. *Int J Radiat Oncol Biol Phys* 2012;83:1047–1054. https://doi.org/10.1016/j.ijrobp.2011.07.039.
[6] Fogliata A, Bergström S, Cafaro I, Clivio A, Cozzi L, Dipasquale G, *et al*. Cranio-spinal irradiation with volumetric modulated arc therapy: a multi-institutional treatment experience. *Radiother Oncol* 2011;99:79–85. https://doi.org/10.1016/j.radonc.2011.01.023.
[7] Lee YK, Brooks CJ, Bedford JL, Warrington AP, Saran FH. Development and evaluation of multiple isocentric volumetric modulated arc therapy technique for craniospinal axis radiotherapy planning. *Int J Radiat Oncol Biol Phys* 2012;82:1006–1012. https://doi.org/10.1016/j.ijrobp.2010.12.033.
[8] Seravalli E, Bosman M, Lassen-Ramshad Y, Vestergaard A, Oldenburger F, Visser J, *et al*. Dosimetric comparison of five different techniques for craniospinal irradiation across 15 European centers: analysis on behalf of the SIOP-E-BTG

(radiotherapy working group). *Acta Oncol* 2018;57:1240–1249. https://doi.org/10.1080/0284186X.2018.1465588.

[9] Myers P, Stathakis S, Mavroidis P, Esquivel C, Papanikolaou N. Evaluation of localization errors for craniospinal axis irradiation delivery using volume modulated arc therapy and proposal of a technique to minimize such errors. *Radiother Oncol* 2013;108:107–113. https://doi.org/10.1016/j.radonc.2013.05.026.

[10] Witztum A, Mandeville HC, Saran FH, Smyth G. Dosimetric effect of setup errors on multiple isocenter volumetric modulated arc radiation therapy for craniospinal axis. *Int J Radiat Oncol Biol Phys* 2014;90:S838–S839. https://doi.org/10.1016/j.ijrobp.2014.05.2408.

[11] Wang K, Meng H, Chen J, Zhang W, Feng Y. Plan quality and robustness in field junction region for craniospinal irradiation with VMAT. *Phys Med* 2018;48:21–26. https://doi.org/10.1016/j.ejmp.2018.03.007.

[12] Ajithkumar T, Horan G, Padovani L, Thorp N, Timmermann B, Alapetite C, *et al*. SIOPE–Brain tumor group consensus guideline on craniospinal target volume delineation for high-precision radiotherapy. *Radiother Oncol* 2018;128:192–197. https://doi.org/10.1016/j.radonc.2018.04.016.

[13] Hoeben BA, Carrie C, Timmermann B, Mandeville HC, Gandola L, Dieckmann K, *et al*. Management of vertebral radiotherapy dose in paediatric patients with cancer: consensus recommendations from the SIOPE radiotherapy working group. *Lancet Oncol* 2019;20:e155–e166. https://doi.org/10.1016/S1470-2045(19)30034-8.

[14] Noble DJ, Ajithkumar T, Lambert J, Gleeson I, Williams MV, Jefferies SJ. Highly conformal craniospinal radiotherapy techniques can underdose the cranial clinical target volume if leptomeningeal extension through skull base exit foramina is not contoured. *Clin Oncol* 2017;29:439–447. https://doi.org/10.1016/j.clon.2017.02.013.

[15] Bedford JL, Lee YK, Wai P, South CP, Warrington AP. Evaluation of the Delta4 phantom for IMRT and VMAT verification. *Phys Med Biol* 2009;54:N167–N176. https://doi.org/10.1088/0031-9155/54/9/N04.

[16] Penagaricano J, Moros E, Corry P, Saylors R, Ratanatharathorn V. Pediatric craniospinal axis irradiation with helical Tomotherapy: patient outcome and lack of acute pulmonary toxicity. *Int J Radiat Oncol Biol Phys* 2009;75:1155–1161. https://doi.org/10.1016/j.ijrobp.2008.12.083.

[17] Wong KK, Ragab O, Tran HN, Pham A, All S, Waxer J, *et al*. Acute toxicity of craniospinal irradiation with volumetric-modulated arc therapy in children with solid tumors. *Pediatr Blood Cancer* 2018;65:e27050. https://doi.org/10.1002/pbc.27050.

[18] Bates JE, Howell RM, Liu Q, Yasui Y, Mulrooney DA, Dhakal S, *et al*. Therapy-related cardiac risk in childhood cancer survivors: an analysis of the Childhood Cancer Survivor Study. *J Clin Oncol* 2019;37:1090–1101. https://doi.org/10.1200/JCO.18.01764.

[19] Shrestha S, Bates JE, Liu Q, Smith SA, Oeffinger KC, Chow EJ, *et al*. Radiation therapy related cardiac disease risk in childhood cancer survivors: updated dosimetry analysis from the Childhood Cancer Survivor Study. *Radiother Oncol* 2021;163:199–208. https://doi.org/10.1016/j.radonc.2021.08.012.

[20] Yock TI, Yeap BY, Ebb DH, Weyman E, Eaton BR, Sherry NA, *et al*. Long-term toxic effects of proton radiotherapy for paediatric medulloblastoma: a phase 2 single-arm study. *Lancet Oncol* 2016;17:287–298. https://doi.org/10.1016/S1470-2045(15)00167-9.

[21] Padovani L, Horan G, Ajithkumar T. Radiotherapy advances in paediatric medulloblastoma treatment. *Clin Oncol* 2019;31:171–181. https://doi.org/10.1016/j.clon.2019.01.001.